Energy 226 (2021) 120379

Contents lists available at ScienceDirect

Energy

journal homepage: www.elsevier.com/locate/energy

Multi-objective wind power scenario forecasting based on PG-GAN

Ran Yuan [a], Bo Wang [a, *], Zhixin Mao [b], Junzo Watada [c]

[a] School of Management and Engineering, Nanjing University, Nanjing, 210093, China
[b] Powerchina Jiangxi Electric Power Construction Co., Ltd, Nanchang, 330001, China
[c] Graduate School of Information, Production and Systems, Waseda University, Kitakyushu, 808-0135, Japan

ARTICLE INFO

Article history:
Received 11 November 2020
Received in revised form
6 March 2021
Accepted 11 March 2021
Available online 18 March 2021

Keywords:
Wind power generation
Scenario forecasting
Progressive growing of generative adversarial networks
Multi-objective optimization

ABSTRACT

Accurate scenario forecasting of wind power is crucial to the day-ahead scheduling of power systems with large-scale renewable generation. However, the intermittence and fluctuation of wind energy bring great challenges to the improvement of prediction accuracy. Aiming at precisely modeling the uncertainty in wind power, a novel scenario forecasting method is proposed in this paper. First, Progressive Growing of Generative Adversarial Networks is leveraged to capture the complex temporal dynamics and pattern correlations. Second, wind power scenarios of the forecast day are achieved by solving a multi-objective scenario forecasting problem with progressive optimization-based Non-dominated Sorting Genetic Algorithm III. Finally, a real wind power dataset and a real power system scheduling problem are applied to justify the effectiveness of the research. Experimental results based on the dataset indicate that our method produces high-quality scenarios with richer details compared with existing research even if the given point forecast is inaccurate. Besides, different amounts of scenarios can be provided without sacrificing time efficiency, which follow the actual trend of wind power consistently and demonstrate great superiority in three evaluation metrics. Moreover, experimental results of the scheduling problem also prove that our method outperforms the others on expected total costs and unmet load amounts.

1. Introduction

With the high penetration of renewable energy, the proportion of wind power continues to grow rapidly all over the world [1]. Wind power is usually considered as non-schedulable due to the strong randomness and intermittence involved, which poses significant challenges to the stability, reliability and security of power systems [2]. Therefore, accurate short-term forecasting of wind power is important and urgent, which can help reduce the wind curtailment and improve the operational efficiency [3]. However, due to the influence of meteorological factors such as temperature and atmospheric pressure, as well as environmental factors such as terrain and topography, high-precision prediction of wind power is intractable and a marked forecasting error exists [4]. In the literature, four approaches are mainly adopted to deal with the stochastic nature of real-world wind power uncertainty, including point forecasting, interval forecasting, probabilistic forecasting, and scenario generation. The widely-used point forecasting approach produces a conditional expectation of wind power output, which belongs to the deterministic prediction [5]. The interval forecasting approach generates the upper and lower bounds of wind power [6], while the probabilistic distribution information for all observations is provided by the probabilistic forecasting approach [7]. Compared with the former three, scenario generation produces time-dependent uncertain information among different look-ahead times [8]. Wherein, the uncertain information can be represented through the collection of multiple deterministic scenarios, referred as to a set of possible time trajectories in nature. The scenario generation methods are of great significance to the optimal operation analysis of power systems with random variables, which provide typical scenarios as input for dynamic decision-making problems (e.g., unit commitment [9], economical dispatch [10]). Meanwhile, scenarios are the ideal tools to visualize the multivariate probabilistic distribution [7]. Because the inherent advantage in capturing the spatial-temporal correlations among multiple wind farms, especially for those which have geographical adjacency, scenario generation methods have received great attention by renewable producers and power system operators.

* Corresponding author.
E-mail addresses: yuanran1222@163.com (R. Yuan), bowangsme@nju.edu.cn (B. Wang), mzx699@vip.sina.com (Z. Mao), junzo.watada@gmail.com (J. Watada).

https://doi.org/10.1016/j.energy.2021.120379
0360-5442/

Specific to the day-ahead wind power scenario generation which is also referred to as scenario forecasting, there are limited studies that have developed systematic schemes for high-quality (i.e., richer details and more consistent trend) scenarios in the case of inaccurate point forecast provided. With this concern, a new method is proposed in this paper based on an improved variant of Generative Adversarial Networks (GAN) [11] called Progressive Growing of Generative Adversarial Networks (PG-GAN) [12] and multi-objective optimization to capture the complex temporal dynamics and diurnal pattern correlations between historical wind power and corresponding point forecast. To the authors' knowledge, this is the first paper that utilizes the GAN-based multi-objective optimization in the scenario forecasting field. Compared with existing research which will be detailed in Section 2 and summarized in Table 1, the novelties and contributions of this paper are mainly threefold:

1) We improve the training procedure of GAN by using PG-GAN. Compared with existing study on scenario generation, our method remarkably promotes the quality of the generated wind power scenarios.
2) A novel output structure of GAN is designed, based on which a complete multi-objective scenario forecasting model is built to better utilize historical data and given point forecast data. In addition, Non-dominated Sorting Genetic Algorithm III (NSGA-III) [13] is improved based on progressive optimization to solve the multi-objective problem.
3) Compared with three benchmark methods, our method shows obvious superiority on several famous scenario evaluation metrics and has better performance when applied to the day-ahead scheduling of power systems. Sensitive analysis on the parameters of the output structure of GAN is also provided. Besides, we prove that the proposed method is capable of generating different amounts of wind power scenarios without sacrificing time efficiency.

The remainder of this paper is organized as follows: Section 2 enumerates and analyzes the existing research. In Section 3, the proposed method is given, including the model used in wind power scenario generation and the detailed framework of multi-objective scenario forecasting. Then in Section 4, we provide the experimental results based on a real dataset to justify the effectiveness of the proposed method. Finally, Section 5 summarizes the conclusions.

2. Literature review

Traditional scenario generation methods are mainly based on the statistical model which is usually used to fit the high-dimensional probabilistic distributions of random variables related to wind energy (e.g., wind speed, wind generation and their forecast errors). In particular, the crucial parameters of statistical distributions are learned and fine-tuned according to the known meteorological information or historical wind power data. For instance, in Ref. [14], a scenario generation method was proposed to characterize the uncertainty of wind power, which is based on the empirical cumulative distribution of forecast errors within a certain forecast bin. In Ref. [15], the multivariate Autoregressive Moving Average (ARMA) was introduced to characterize the spatial-temporal correlations of wind speed distribution by employing the variance-covariance matrix. Copula methods including single copula [16], pair copula [17] and vine copula [18], are the main approaches to describe the correlation structure among multiple wind farms. Under the framework of Copula methods, the spatial-temporal interdependence structure of wind power output was modeled by the covariance matrix, then some inverse transformation sampling techniques (e.g. Monte Carlo simulation) were used to generate the scenarios. To relieve the computation burden of subsequent stochastic optimization, scenario reduction based on sub-modularity [19], correlation loss [20] and heuristic search [21] have been developed to reduce the number of scenarios. However, it is difficult to capture the correlated movements of multiple time series of wind power scenarios by using low-order statistical models above, which rely heavily on the accuracy of distribution assumption. In addition, sampling efficiency and scenario reduction effectiveness are often limited to

Table 1
Comparative analysis of existing scenario generation & forecasting methods.

Methods	Algorithms and Literature	Advantages	Disadvantages
Statistical Methods	• Empirical Cumulative Distribution of Forecast Error [14] • Multivariate Autoregressive Moving Average (ARMA) [15] • Copula Functions including Single Copula [16], Pair Copula [17] and Vine Copula [18]	• Use low-order statistical models, easy to understand and compute. • Low computational efforts due to the simplified estimation.	• Need probabilistic assumptions in advance. • Cumbersome scenarios sampling process. • Difficult to guarantee scenarios diversity.
Machine Learning Methods	• Artificial Neural Networks [22,23] • Quantile Regression Convolutional Neural Networks (QRCNN) [24] • Radial Basis Function Neural Networks (RBFNN) [25]	• Non-parametric, do not need any probabilistic assumption. • Feedforward neural network, easy to scale.	• Complex data feature extraction and parameter tuning. • Prone to overfitting.
GAN-based Methods	• Wasserstein GAN (WGAN) and Conditional GAN (CGAN) [27] • Bayesian GAN [28] • Improved WGAN-GP [29] • GAN with Variational Inference [30]	• Model-free, without any assumption of distribution shape. • Data-driven, generate scenarios directly from historical data. • Do not need probabilistic sampling. • Better flexibility for extrapolation.	• Unstable training. • Unable to generate day-ahead scenarios.
	• CGAN followed by Single-objective Optimization [31] • WGAN-GP and Convolutional Neural Networks Classifier [32] • Conditional WGAN-GP and Support Vector Classifier [33] • Sequence GAN (SeqGAN) [34]		• Rely on the accuracy of day-ahead point forecast or classifier. • Without differentiating diurnal patterns of consecutive days.

the actual environment, resulting in scenarios diversity cannot be always guaranteed.

To address the defect of statistical models, non-parametric methods based on machine learning have been proposed to generate scenarios. In Ref. [22], an iterative neural network was established to output wind scenarios by generating step-ahead forecasts and random errors, and a similar way was adopted in Ref. [23]. In Ref. [24], the detailed quantiles of wind power prediction were obtained by Quantile Regression Convolutional Neural Networks (QRCNN) and then approximated as a cumulative distribution function of wind power. Furthermore, a Radial Basis Function Neural Networks (RBFNN)-based probabilistic prediction model for wind power scenarios was proposed in Ref. [25]. Wind power usually shows strong volatility and irregularity that represent the high dimensional nonlinear and non-stationary relations between generation level and relevant influence factors [26]. These non-parametric approaches therefore need to be designed in a complicated way to improve their data mapping capacities. Nevertheless, a more complicated structure also means that the feature extraction and parameter tuning processes are more trivial and time-consuming.

Recently, some literature focused on the application of GAN on scenario generation. As one of the unsupervised generative models, GAN can effectively avoid complex feature extraction and cumbersome manual labeling process, which has been widely used in image-to-image translation [35], natural language processing [36] and other fields to produce fairly realistic samples like the original data. A detailed introduction about GAN is provided in Subsection 3.1.1. With regard to the wind power scenario generation, while the potential benefits of wind-energy-to-wind-power physical process are clear, a major barrier in its implementation comes from the uncertainty of meteorological variable prediction (especially wind speed) [37]. Therefore, data-driven approaches using GAN and its improved variants were developed to produce scenarios directly based on historical data related to wind power. In Ref. [27], Wasserstein GAN (WGAN) and Conditional GAN (CGAN) were adopted to generate wind and photovoltaic power scenarios based on weather event conditions. In order to identify different patterns in historical data, Bayesian GAN was developed to generate renewable scenarios [28]. When training GAN, instability and saturation phenomena tend to occur, incurring severe mode collapse [38]. Concretely speaking, it will lead to wind power scenarios focusing on a certain historical generation pattern obviously and lack of diversity, which holds back the capacity of scenarios for characterizing wind uncertainty. To circumvent the problem, Ref. [29] added a consistency term to the loss function of Wasserstein GAN with Gradient Penalty (WGAN-GP), thus improving both training stability and scenario quality. In Ref. [30], Variational Inference (VI) was introduced to the traditional GAN structure to achieve more precise reflection of the dynamic patterns of wind and photovoltaic power. However, scenarios generated by the above GAN-based methods may represent wind power profile of any future day, which cannot be directly applied to the day-ahead scheduling of power systems.

From the perspective of decision making and risk assessment, it is necessary to produce accurate day-ahead scenarios given any known conditions (e.g., numerical weather prediction, day-ahead point forecast), which is referred to as "***scenario forecasting***". For the sake of distinction, we still use the phrase "***scenario generation***" in the following sections, but only describe the process of producing scenarios randomly by GAN. Research about GAN-based wind power scenario forecasting is still in its infancy. In Ref. [31], the work of [27] was extended to a scenario forecasting approach by formulating an optimization problem aiming at generating scenarios conditioned on the corresponding day-ahead point forecast. In addition, some literature proposed to train a high-performance classifier firstly to predict the weather category [32] or the forecast error label [33] of the forecast day, then use GAN to generate a series of scenarios under the classification. In Ref. [34], a novel GAN structure based on Reinforcement Learning named SeqGAN was developed to directly predict the time series of forecast errors or wind generation conditioned on the corresponding input sequence data of previous days. Despite the aforementioned recent advances, the quality of forecasted scenarios relies greatly on the accuracy of day-ahead point forecast or pretrained classifier, which sometimes leads to unreliable results and thereby increasing the operational risk of power systems (e.g. load shedding and delivery failures). Meanwhile, the underlying wind power diurnal patterns of several consecutive days have not been quantitatively evaluated by existing research in an in-depth and comprehensive way. Accordingly, we try to develop a new method with better performance to provide high-quality day-ahead wind power scenarios for the characterization of uncertainty in power system operations.

3. Proposed method

In this research, we propose a novel method for high-quality wind power scenario forecasting which includes two stages: the stage of scenario generation based on PG-GAN, and the stage of scenario forecasting based on multi-objective optimization. Conceptually, "rough" scenarios are firstly produced at the scenario generation stage by feeding random latent vectors to the generator of PG-GAN, which are further optimized at the scenario forecasting stage by applying the known information specific to the forecast day (i.e. historical data and given point forecast of wind power). The flowchart of the proposed method is given in Fig. 1.

In the training process, suppose that we have totally M_{train}-days observations on the historical wind production data, and the corresponding day-ahead point forecast results provided by any method, which can be expressed as:

- M_{train}-days historical wind power data: $\mathbb{W}_{\text{H}} = \{W_{\text{H}}^1, \cdots, W_{\text{H}}^{M_{\text{train}}}\}$.
- Corresponding M_{train}-days wind power point forecast data: $\mathbb{F}_{\text{H}} = \{F_{\text{H}}^1, \cdots, F_{\text{H}}^{M_{\text{train}}}\}$.

In the phase of scenario generation, our model is trained based on $\mathbb{W}_{\text{H}}$ and $\mathbb{F}_{\text{H}}$, to generate the following scenarios simultaneously:

- Wind power scenarios of n-consecutive-days: $\mathbb{W}_{\text{G}} = \{W_{\text{G}}^1, \cdots, W_{\text{G}}^n\}$, where $n \ll M_{\text{train}}$.
- Corresponding day-ahead wind power point forecast scenarios of n-consecutive-days: $\mathbb{F}_{\text{G}} = \{F_{\text{G}}^1, \ldots, F_{\text{G}}^n\}$, again $n \ll M_{\text{train}}$.

The details of $\mathbb{W}_{\text{G}}$ and $\mathbb{F}_{\text{G}}$ are enriched by PG-GAN during the progressive training process. Detailed information about scenario generation is provided in Subsection 3.1.

Then in the phase of scenario forecasting such as for the forecast day d, a multi-objective optimization model is formulated to minimize the difference between the generated scenarios ($\mathbb{W}_{\text{G}}$, $\mathbb{F}_{\text{G}}$) and the available data information related to d, which includes the previous $(n-1)$-days historical wind power data before d and the corresponding n-days wind power point forecast data including the forecast day d. Compared with single-objective optimization which regards the available data as a whole, our method makes a division by day, which is intended to differentiate diurnal patterns of wind power in several consecutive days and capture the potential day-ahead pattern. Specifically, the data matching process of each day

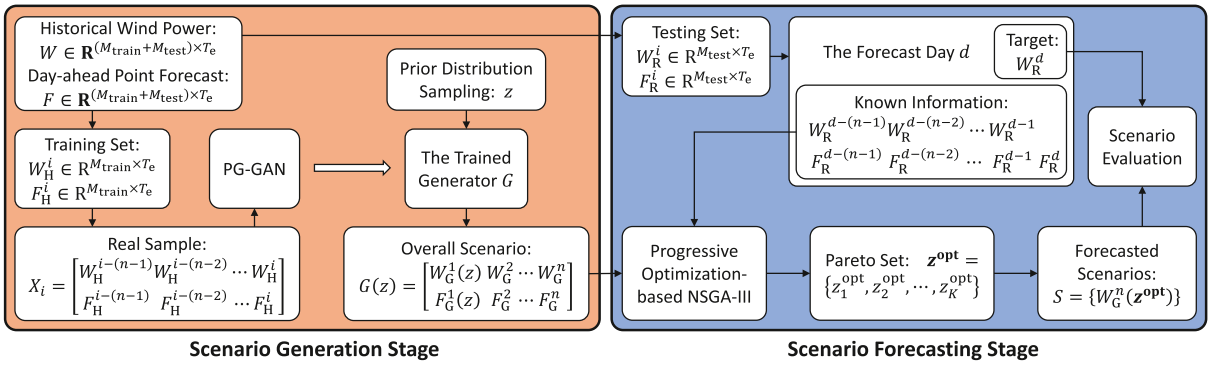

Fig. 1. The flowchart of the proposed method.

can be treated as a separate objective, thus resulting in multi-objective optimization. Moreover, progressive optimization-based NSGA-III (PO-NSGA-III) is developed to efficiently solve the proposed multi-objective problem. The details of scenario forecasting is provided in Subsection 3.2. It is noteworthy that this paper focus specially on the wind power, but the general framework of the proposed method can clearly extend to other renewable generation like photovoltaic. Since there is no need to make explicit assumptions on renewable probability distributions, the proposed method can be carried out to produce day-ahead scenarios as long as sufficient historical data of interest is available.

3.1. Wind power scenario generation

In this subsection, the method for wind power scenario generation is given. We first review the original GAN, then present the output scenario structure of our GAN, and finally introduce how the PG-GAN is used to enrich the scenario details.

3.1.1. Generative Adversarial Networks

GAN is a deep generative model consisting of two competing neural networks: the generator G and the discriminator D, as shown in Fig. 2. G learns the training data distribution and generates a sample $G(z)$, where the input z is a latent vector variable sampled from a simple prior random distribution $p_z(z)$ (e.g., Gaussian, Uniform). And D tries to discriminate the generated sample $G(z)$ from a real sample X, which can be treated as a binary classifier that outputs the probability regarding the real sample. The two models are trained simultaneously by updating the network weights in an alternating manner, and their training procedure can be treated as a two-player minmax game with the objective function formulated as follows:

$$\min_G \max_D V(G,D) = \mathbb{E}_{z\sim p_z(z)}[\log(1-D(G(z)))] + \mathbb{E}_{X\sim p_X(X)}[\log D(X)], \tag{1}$$

where $p_X(X)$ refers to the real data distribution. The training process finishes when Nash equilibrium is achieved between G and D,

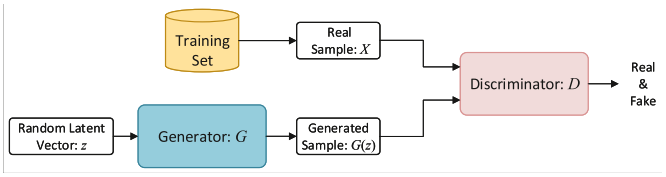

Fig. 2. The structure of GAN.

then G can be used to directly generate synthetic samples without explicitly specifying a model or fitting probability distributions.

3.1.2. Scenario structure

Day-ahead point forecast is mostly based on the meteorological prediction, which is conducive to the high-quality scenario forecasting when taking the correlations between historical wind power and point forecast into consideration. Based on this, we try to use GAN to output an overall scenario $G(z)$ composed of n-consecutive-days wind power scenario $\mathbb{W}_G(z)$ and corresponding point forecast scenario $\mathbb{F}_G(z)$, each of which is further divided into n sub-scenarios by day (in total $2n$ sub-scenarios), as shown in Fig. 3(b). In essence, each sub-scenario is a T_e-dimensional vector, where T_e is the number of time slots included in one day. The detailed structure of the overall scenario $G(z)$ can be written as:

$$G(z) = \begin{bmatrix} \mathbb{W}_G(z) \\ \mathbb{F}_G(z) \end{bmatrix} = \begin{bmatrix} W_G^1(z) & W_G^2(z) & \cdots & W_G^n(z) \\ F_G^1(z) & F_G^2(z) & \cdots & F_G^n(z) \end{bmatrix}. \tag{2}$$

The most obvious advantage of this scenario structure is to enable GAN to learn and reflect the deviation level between wind power and point forecast, i.e., we hope to generate a set of plausible future wind power scenarios even if the given future point forecast is inaccurate. In this sense, we would like to make full use of GAN's ability to capture the following four types of correlations:

- Internal temporal dependence within each sub-scenario, such as $W_G^1(z)$.
- Daily pattern correlations among $\mathbb{W}_G(z)$, such as $W_G^1(z)$ and $W_G^2(z)$.
- Daily pattern correlations among $\mathbb{F}_G(z)$, such as $F_G^1(z)$ and $F_G^2(z)$.
- Daily pattern correlations between $\mathbb{W}_G(z)$ and $\mathbb{F}_G(z)$, such as $W_G^1(z)$ and $F_G^1(z)$.

Accordingly, as shown in Fig. 3(a), the real sample can be integrated by every n consecutive days from $\mathbb{W}_H$ and:

$$X_i = \begin{bmatrix} W_H^{i-(n-1)} & W_H^{i-(n-2)} & \cdots & W_H^i \\ F_H^{i-(n-1)} & F_H^{i-(n-2)} & \cdots & F_H^i \end{bmatrix}, \tag{3}$$

where X_i denotes the i^{th} real sample consisting of wind power and corresponding point forecast of the day i as well as its previous $n-1$ days. The value of i herein takes from $\{n, n+1, \cdots, M_{\text{train}}\}$, thus a total of $M_{\text{train}} - n + 1$ real samples can be obtained to train the GAN model.

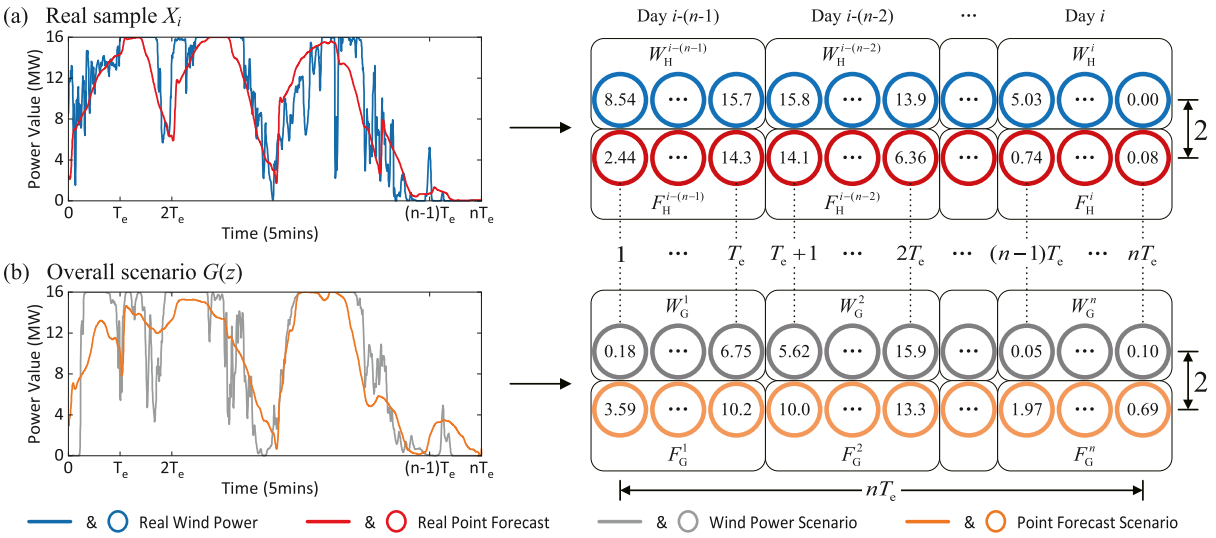

Fig. 3. The structure of i^{th} real sample X_i (a) and overall scenario $G(z)$ (b). The wind power (blue), given point forecast (red), generated wind power scenarios (gray) and generated point forecast scenarios (orange) of n-consecutive-days in each time slot with power values are exhibited in the form of solid lines and hollow circles. The time slots $\{1, 2, \cdots, nT_e\}$ are also marked in the graph, where n is the number of consecutive days and T_e is the number of time slots included in one day. (For interpretation of the references to colour in this figure legend, the reader is referred to the Web version of this article.)

3.1.3. Progressive Growing of GAN

It is widely acknowledged that the original GAN has several defects, such as gradient vanishing and mode collapse, which severely restrict its applications, thus resulting in insufficient details and low diversity of the generated scenarios. In this paper, we overcome the above defects by improving the training procedure motivated by PG-GAN which has been successfully applied in the field of high-resolution face images generation. As shown in Fig. 4(a), we start the training procedure with a relatively low scenario resolution $2 \times T_{\min}$ (e.g. 2×9) where 2 indicates the two types of scenarios included in the overall scenario, and we use T to express the resolutions between $T_{\min}$ and $T_{\max}$. Then we gradually increase the resolution by adding new network layers to D and G, and finally end with the ultimate scenario resolution $2\times T_{\max}$ (e.g. 2×2304). Herein, the value of $T_{\max}$ is determined by:

$$T_{\max} = n^{*}T_e, \tag{4}$$

where T_e is the number of time slots included in one day and n has the same meaning as Equation (2). We adopt the state-of-the-art loss function WGAN-GP, which replaces the weight clipping in WGAN with a gradient penalty term:

$$\begin{aligned} L_D &= \mathbb{E}_{z\sim p_z(z)}[D(G(z))] - \mathbb{E}_{X\sim p_X(X)}[D(X)] + \lambda \mathbb{E}_{\widehat{X}\sim p_{\widehat{X}}(\widehat{X})}\left[\left(\left\|\nabla_{\widehat{X}} D\left(\widehat{X}\right)\right\|_2 - 1\right)^2\right], \\ L_G &= -\mathbb{E}_{z\sim p_z(z)}[D(G(z))], \\ \widehat{X} &= \varepsilon X + (1-\varepsilon)G(z),\ \varepsilon \sim U[0,1], \end{aligned} \tag{5}$$

where L_D and L_G refer to the loss function of D and G respectively, λ is a weighting parameter that controls the impact of gradient penalty term.

In order to stabilize the training process, a smooth fade-in transition process is integrated into PG-GAN when doubling the resolution, as shown in Fig. 4(b). In addition, some significant training tricks (e.g., equalized learning rate, pixel-wise feature vector normalization [12]) are applied to restrict the escalation of signal magnitudes, which can effectively avoid disorder competition between G and D. To increase the variation of scenarios, a mini-batch standard deviation layer [12] is added into the end of D. Employing the learning process of PG-GAN enables our networks to capture the characteristics of scenarios from coarse to fine thus producing high-quality scenarios.

3.2. Wind power scenario forecasting

In this subsection, a multi-objective wind power scenario forecasting model is proposed, whereafter a progressive optimization-based NSGA-III is designed as the solution algorithm of the model.

3.2.1. Problem formulation

After the progressive training of GAN is completed, when some latent variable z is input to the generator of PG-GAN, we can obtain an overall scenario $G(z)$ consisting of $2n$ sub-scenarios that reflect n-consecutive-days wind power and corresponding point forecast, as shown in Equation (2). Due to the unsupervised characteristics, the wind power scenarios obtained by PG-GAN in Subsection 3.1 lack clear pertinence about the forecast day, i.e., they may represent wind power profile of any future day, which cannot be directly applied to the day-ahead scheduling of power systems. Therefore, the following approach is used to improve the output of PG-GAN, so that matching the feature of the forecast day. Specifically, for the forecast day d, we have the previous $(n-1)$-days wind power data before d, denoted as $\{W_R^{d-(n-1)}, \cdots, W_R^{d-1}\}$. Moreover, we have the

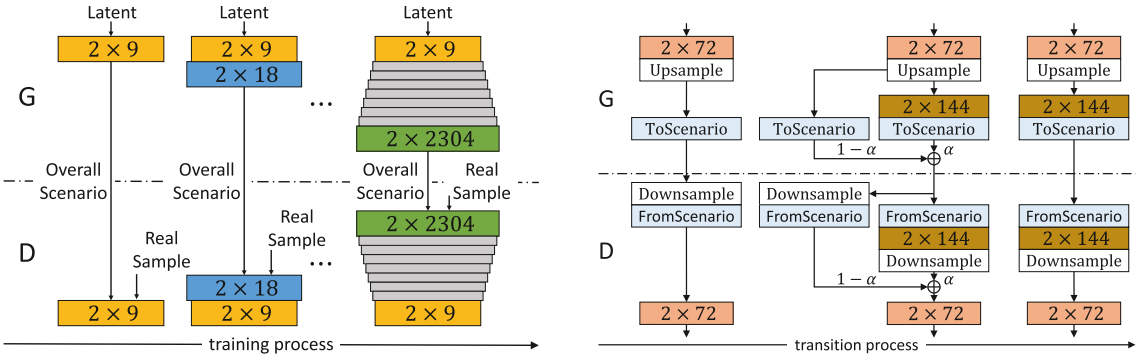

(a) Progressive training process (b) Smooth fade-in transition process

Fig. 4. The mechanism of PG-GAN. Progressive training process (a), here $2 \times T$ ($T = 9, 18, \cdots, 2304$) refers to a network block composed of two cascaded convolutional layers operating on $2 \times T$ scenario resolution. Smooth fade-in transition process (b), this example illustrates the transition process of scenario resolution from $2\times$ 72 to $2\times$ 144. The parameter α gradually increases from 0 (left) to 1 (right) during the transition period. The upsample and downsample operations are used for doubling and halving scenario resolution, respectively.

corresponding n-days wind power point forecast data including the forecast day, which can be represented as $\{F_{\mathrm{R}}^{d-(n-1)}, \cdots, F_{\mathrm{R}}^{d}\}$. Note that wind power of the forecast day W_{R}^{d} is unknown, which is the target of our scenario forecasting. In this paper, the purpose is to find the optimal z that minimizes the difference between $G(z)$ and the above available information related to d. Based on this consideration, the objectives to be optimized are summarized as follows:

$$O_i(z) = \left\{ \left|\left| W_{\mathrm{G}}^{i}(z) - W_{\mathrm{R}}^{d-(n-i)} \right|\right| + \beta \left|\left| F_{\mathrm{G}}^{i}(z) - F_{\mathrm{R}}^{d-(n-i)} \right|\right| \right. \\ \left. \times \left| \text{if } i = 1, 2, \cdots, n-1 (1+\beta)^{*} \left|\left| F_{\mathrm{G}}^{i}(z) - F_{\mathrm{R}}^{d-(n-i)} \right|\right| \right| \quad \text{if } i = n, \tag{6}$$

where $||\cdot||$ denotes the Mean Square Error (MSE), and the confidence factor β measures the degree to which we trust the point forecast. Note that the number of objectives is determined by the consecutive days in $G(z)$. Therefore, a generalized n-objective scenario forecasting problem can be realized as follows when $G(z)$ consists n-consecutive-days:

$$\min_{z} \begin{cases} O_1 &= \left|\left| W_{\mathrm{G}}^{1}(z) - W_{\mathrm{R}}^{d-(n-1)} \right|\right| + \beta\, F_{\mathrm{G}}^{1}(z) - F_{\mathrm{R}}^{d-(n-1)} \\ O_2 &= W_{\mathrm{G}}^{2}(z) - W_{\mathrm{R}}^{d-(n-2)} + \beta \left|\left| F_{\mathrm{G}}^{2}(z) - F_{\mathrm{R}}^{d-(n-2)} \right|\right| \\ &\vdots \\ O_{n-1} &= \left|\left| W_{\mathrm{G}}^{n-1}(z) - W_{\mathrm{R}}^{d-1} \right|\right| + \beta \left|\left| F_{\mathrm{G}}^{n-1}(z) - F_{\mathrm{R}}^{d-1} \right|\right| \\ O_n &= (1+\beta)^{*} \left|\left| F_{\mathrm{G}}^{n}(z) - F_{\mathrm{R}}^{d} \right|\right| \end{cases} \\ \text{s.t.} \quad z \in p_z(z) \tag{7}$$

Suppose that z_i^{opt} is the i^{th} pareto optimal solution, and $\mathbf{z}^{\mathrm{opt}} = \{z_1^{\mathrm{opt}}, z_2^{\mathrm{opt}}, \cdots, z_K^{\mathrm{opt}}\}$ is the pareto set of the problem, which includes K solutions, then we can obtain the corresponding wind power sub-scenario set:

$$S = \left\{ W_{\mathrm{G}}^{n}(\mathbf{z}^{\mathrm{opt}}) \right\}, \tag{8}$$

which can be regarded as the K forecasted wind power scenarios of the forecast day d.

Algorithm 1
Progressive Optimization-based NSGA-III for Scenario Forecasting.

Input: The proposed wind power scenario forecasting problem $\Omega^{2\times T_{\max}}$; Population size n_{pop}; Crossover rate α_1, mutation rate α_2; Maximum iteration n_{iter};
Output: The pareto set of $\Omega^{2\times T_{\max}}$: $\mathbf{z}^{\mathrm{opt}} = \mathbf{z}^{2\times T_{\max}}$;
Set initial population as $P_{\mathrm{init}} = \{z_1^{\mathrm{init}}, z_2^{\mathrm{init}}, \cdots, z_{n_{\mathrm{pop}}}^{\mathrm{init}}\}$, where z_i is randomly sampled from prior distribution $p_z(z)$.
for $T = T_{\min}, 2T_{\min}, \cdots, T_{\max}$ **do**
  if $T = T_{\min}$ **then**
    $P_{\mathrm{prophet}} = P_{\mathrm{init}}$
  else
    $P_{\mathrm{prophet}} = \mathbf{z}^{2\times(T/2)}$
  end if
  # Optimize the scenario forecasting problem on $2 \times T$ *resolution derived from* $\Omega^{2\times T_{\max}}$: $\Omega^{2\times T}$
  for $t = 1$ to $n_{\mathrm{iter}} - 1$ **do**
    $P_1 = P_{\mathrm{prophet}}$
    Get the t-th offspring population: $Q_t = Crossover_{\alpha_1} + Mutation_{\alpha_2}(P_t)$
    Combine parent and offspring population: $R_t = P_t \cup Q_t$
    Calculate objective values of R_t on $\Omega^{2\times T}$.
    $P_{t+1} = Non\text{-}dominated\text{-}sort + Normalize + Associate + Niche\text{-}preserve\ (R_t)$
  end for
  Extract all non-dominated solutions in the $2 \times T$ resolution stage from $P_{n_{\mathrm{iter}}}$: $\mathbf{z}^{2\times T} = \{z_1^{2\times T}, z_2^{2\times T}, \cdots, z_{n_T}^{2\times T}\}$
  if $n_T < n_{\mathrm{pop}}$ and $T < T_{\max}$
    Supplement insufficient $(n_{\mathrm{pop}} - n_T)$ individuals with randomly samples from $p_z(z)$: $\mathbf{z}^{2\times T} = \mathbf{z}^{2\times T} \cup \mathbf{z}^{\mathrm{random}}$
  end if
end for

3.2.2. Progressive optimization-based NSGA-III

To tackle the above n-objective wind power scenario forecasting problem, we consider using NSGA-III which has been proven effective in solving high-dimensional multi-objective problems with the objective number greater than three. The algorithm mainly includes four major parts, i.e., non-dominated-sorting, normalization, association and niche-preservation. Due to the space limits, we omit the detailed knowledge of NSGA-III. The readers are encouraged to refer to Ref. [13] for the details. Generally, when processing high-dimensional variables, the performance of evolutionary algorithms is particularly sensitive to their parameter settings (e.g., crossover rate, mutation rate, etc.), resulting in the drawbacks of being easily trapped in local optimality and poor convergence.

Motivated by the progressive learning of PG-GAN, we improve

NSGA-III based on a progressive optimization manner to overcome the above drawbacks when solving model (7), which is summarized in Algorithm 1. In detail, we construct an initial population of PO-NSGA-III in which each individual is encoded by a latent vector z sampled from the prior distribution $p_z(z)$. The whole optimization process of scenario forecasting is divided into several stages $(2\times T_{\min},\cdots,2\times T_{\max})$ by the resolution. Accordingly, the proposed problem $\Omega^{2\times T_{\max}}$ in model (7) is adjusted to a relatively low-dimensional problem $\Omega^{2\times T}$ through downsampling techniques at each stage, where $2\times T$ indicates the current resolution of overall scenario. Then, an overall scenario with resolution $2\times T$ can be produced using the proposed PG-GAN model for each individual, and n objective values can be calculated by the derived problem $\Omega^{2\times T}$. When the optimization in the previous stage is completed, we obtain a population consisting of individuals corresponding to all non-dominated solutions, which is regarded as the prophet population of the next stage. In order to ensure the consistency of population number at each stage, insufficient part will be supplemented with randomly sampled individuals from $p_z(z)$, which can mitigate the local convergence problem to some extent. In summary, progressive optimization makes the solution process of the proposed high-dimensional wind power scenario forecasting problem mostly completed in a low-dimensional space, which greatly accelerates the population convergence without losing the diversity of solutions.

4. Results

In this section, the effectiveness of the proposed approach is exemplified by a series of experiments based on a real dataset. We first exhibit the detailed progressive training process of the proposed model, which demonstrates that as the resolution increases, the generated scenarios gradually learn more details of the real samples, thus becoming more realistic and indistinguishable. Then, the progressive optimization results of scenario forecasting are given. The statistic properties of the scenarios and the performance in real day-head scheduling of power systems are analyzed and compared.

4.1. Data description

We use the same dataset in Ref. [27] to evaluate the performance of our approach. The dataset includes wind power and corresponding day-ahead point forecast data of 5-min granularity from Jan. 1st, 2007 to Dec. 31st, 2013 in the State of Washington, which is collected from the NREL Wind Integration Dataset [39]. For the purpose of this study, we integrate the data of every 8 consecutive days (in total 2304 time slots) as an experimental sample, and all values in the dataset are normalized to $[-1,1]$ by the nominal capacity (NC, in this study, NC $=$ 16 MW) of the wind farm. Considering the time horizon of NREL dataset, a relatively suitable division of the dataset is determined through preliminary analysis, that is, the last two-month data from Nov. 1st to Dec. 31st, 2013 is used for testing and the remaining is used for training. Additionally, forecast errors are calculated as the difference between the actual power and point forecast values, thus a greater error value representing the point forecast underestimated the actual wind production. To illustrate, the distributions of forecast errors for the training set and testing set are shown in Fig. 5. Statistical characteristics of forecast errors, including mean, standard deviation, maximum and minimum, are also listed in the histograms. It is not hard to find that wind power data with absolute forecast error more than 2 MW account for almost 40% of total counts, indicating significant forecast errors exist in NREL dataset.

Besides, the proposed approach is compared with three benchmark scenario forecasting methods including Chen's Method [31], Vine Copula [18], and Kernel Density Estimation (KDE) [40]. Chen's Method, which has been proven to outperform the conventional Gaussian Copula method, adopts the GAN-based scenario generation approach proposed in Ref. [27] to generate two-consecutive-day wind power scenarios randomly, then performs single-objective scenario forecasting based on the given day-ahead point forecast and the actual power of previous day. In Vine Copula and KDE, wind power probabilistic distribution is firstly modeled in parametric and non-parametric manners respectively, then appropriate inverse transformation sampling techniques are adopted to generate scenarios from the probabilistic distribution. All experiments were implemented using Python with Tensorflow framework on the hardware platform equipped with Intel Core i7-8700 3.2-GHz CPU, 16G RAM and NVIDIA GeForce GTX 1660 GPU.

4.2. Evaluation metrics

The commonly used criteria such as mean absolute error (MAE) and root mean squared error (RMSE) are suitable for deterministic forecasting, but might be limited in the scenario forecasting evaluation with uncertainty. In fact, high-quality scenarios should not only meet calibration requirements but also exhibit sufficient diversity to cover a realistic range of possible wind power realizations. Hence, we introduce three evaluation metrics to assess the quality of scenario forecasting, which include the Energy Score (ES) [41], Brier Score (BS) [42], and Pinball Score (PB) [43].

ES is a multivariate skill, negatively-oriented score, which takes into account the dependency structures and quantifies both the reliability (accuracy) and sharpness (spread) of a scenario set [41]. ES is applied to all the variables at the same time to capture the correlation, which can be computed as:

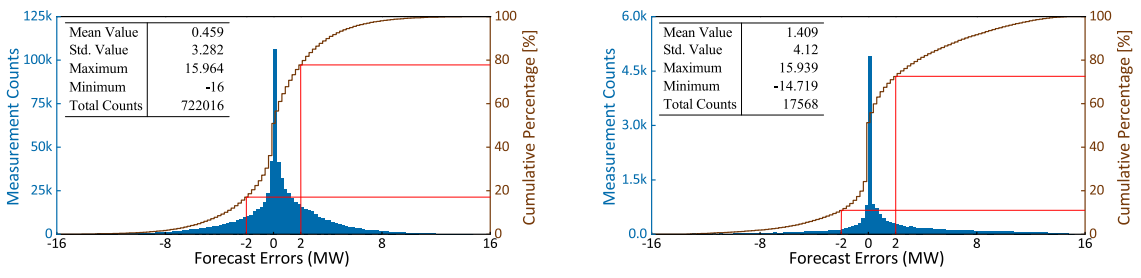

(a) Training set (b) Testing set

Fig. 5. Distributions of wind power forecast errors for NREL 5-min dataset in the training (a) and testing (b) set.

Table 2
Definitions of BS events.

No.	Event	Definition
1	Up-Ramp	$+10\% \times$ NC in 1 h
2	Down-Ramp	$-10\% \times$ NC in 1 h
3	Long-High	$\geq 80\% \times$ NC for 1 h
4	Long-Low	$\leq 5\% \times$ NC for 1 h

$$\mathrm{ES} = \frac{1}{T_e}\sum_{t=1}^{T_e}\left[\frac{1}{K}\sum_{m=1}^{K}\left|\left|s_t - S_{m,t}\right|\right|_2 - \frac{1}{2K^2}\sum_{m=1}^{K}\sum_{n=1}^{K}S_{m,t} - S_{n,t}{}_2\right], \tag{9}$$

where s_t denotes the value of the realized trajectory s (in this study, $s = W_R^d$) in time slot t, and $S_{m,t}$, $S_{n,t}$ denote the m^{th}, n^{th} scenario in time slot t of the forecasted scenario set S.

BS is an index presented in Ref. [42] to evaluate the ability of scenarios to mimic specific statistic features (called events) of the stochastic behaviors of wind power. It is a negatively-oriented metric defined as:

Table 3
Network structure of the proposed GAN model.

Block No.	Generator G	Discriminator D
1	Input, 128	Input, $2 \times 2304 \times 1$
	FC, $2 \times 9 \times 128$	Conv*, $2 \times 2304 \times 128$
	Conv, $2 \times 9 \times 128$	Conv, $2 \times 2304 \times 128$
	Conv, $2 \times 9 \times 128$	Conv, $2 \times 2304 \times 128$
2	Up, $2 \times 18 \times 128$	Down, $2 \times 1152 \times 128$
	Conv, $2 \times 18 \times 128$	Conv, $2 \times 1152 \times 128$
	Conv, $2 \times 18 \times 128$	Conv, $2 \times 1152 \times 128$
⋮	⋮	⋮
8	Up, $2 \times 1152 \times 128$	Down, $2 \times 18 \times 128$
	Conv, $2 \times 1152 \times 128$	Conv, $2 \times 18 \times 128$
	Conv, $2 \times 1152 \times 128$	Conv, $2 \times 18 \times 128$
9	Up, $2 \times 2304 \times 128$	Down, $2 \times 9 \times 128$
	–	MSD, $2 \times 9 \times 128$
	Conv, $2 \times 2304 \times 128$	Conv, $2 \times 9 \times 128$
	Conv, $2 \times 2304 \times 128$	Conv, $2 \times 9 \times 128$
	Conv*, $2 \times 2304 \times 1$	FC, 1

[FC]: Fully Connected layer. [Conv]/[Conv*]: Convolutional layer with kernel size of 2×9 / 1×1.
[MSD]: Minibatch Standard Deviation layer. [Up]/[Down]: Upsample/Downsample using bilinear interpolation.
[*Height* × *Width* × *Channels*] or [*Neurons*]: Output Shape.

$$\mathrm{BS} = \frac{1}{T_e}\sum_{t=1}^{T_e}\left(\mathbb{E}[g_t(S;\theta)] - g_t(s,\theta)\right)^2, \tag{10}$$

where θ denotes the parameter set related to the event of interest, and $g_t(\cdot;\theta)$ indicates whether the event in the forecasted scenarios set S or realized trajectory s occurs in time slot t, which takes the binary value in $\{0,1\}$. BS is an application-oriented approach to the evaluation of scenarios and its value drastically depends on the selection of predefined events. For power system scheduling, operators often focus on both large ramps events and long-lasting events. Hence, we consider defining four specific events: (i) Up-Ramp, (ii) Down-Ramp, (iii) Long-High, and (iv) Long-Low. Based on [41,42], detailed quantitative definitions are listed in Table 2.

PB is another negatively-oriented score widely used in the field of statistics and machine learning. It is a quantile-based metric which measures the distance between a series of forecasted quantiles and corresponding observations [43]. In this paper, we mainly employ PB to assess the marginal properties of the forecasted scenarios. The definition of PB is:

$$\begin{aligned}\mathrm{PB} &= \frac{1}{T_e}\sum_{t=1}^{T_e}\left[\frac{1}{|\Phi|}\sum_{\tau\in\Phi}\mathrm{PB}_{\tau,t}\right],\\ \mathrm{PB}_{\tau,t} &= \begin{cases}\tau\left(s_t - S_t^\tau\right), & S_t^\tau < s_t\\ (1-\tau)\left(S_t^\tau - s_t\right), & S_t^\tau \geq s_t\end{cases},\end{aligned} \tag{11}$$

where τ is the quantile level obtained from a specific set Φ, here we define $\Phi = \{0.01, 0.02, \cdots, 0.99\}$, and S_t^τ represents the τ-quantile value of the forecasted scenarios set S in t.

4.3. Training and parameter settings

Recall the structure of PG-GAN in Fig. 4(a), we start training our GAN model from the minimum scenario resolution of 2×9 ($T_{\min} = 9$), and gradually double the resolution by adding new layers to D and G until reaching the ultimate resolution of 2×2304 ($T_{\max} = 2304$). The granularity of the experimental dataset is 5 min, thus 288 time slots are included in one day ($T_e = 288$). Therefore, we can use GAN to generate overall scenarios reflecting both the wind power and point forecast profiles of $2304/288 = 8$ consecutive days ($n = 8$). Detailed network structures of the proposed GAN with the ultimate resolution are listed in Table 3. We train the

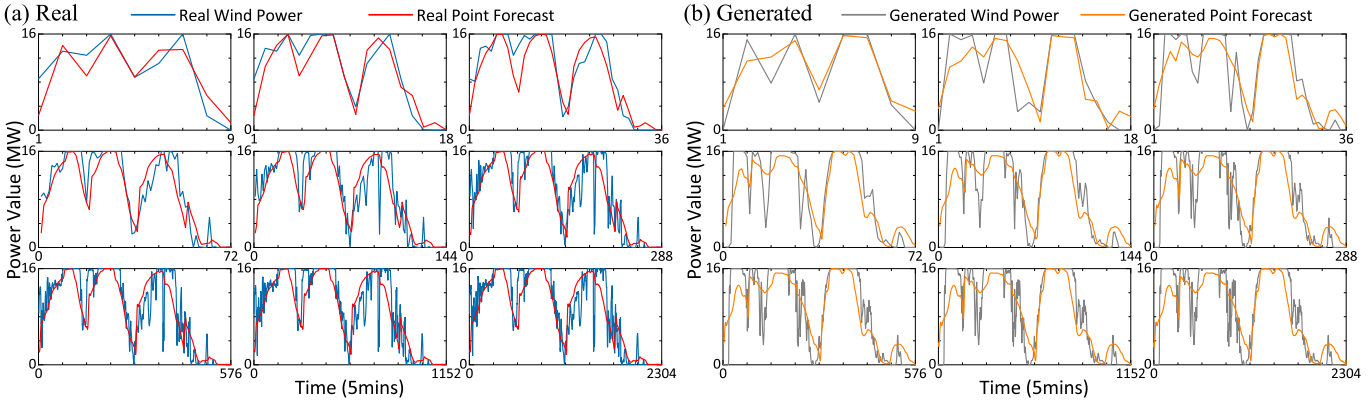

Fig. 6. Comparison of real samples (a) and overall scenarios generated by our GAN model (b) in all resolution dimensions (i.e., $2 \times 9, \cdots, 2 \times 2304$). For each resolution, wind power curve (blue or gray) and corresponding point forecast curve (red or orange) are included. (For interpretation of the references to colour in this figure legend, the reader is referred to the Web version of this article.)

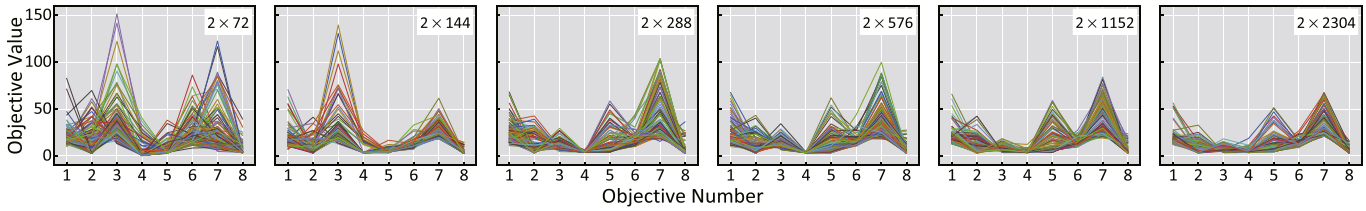

Fig. 7. Objective value paths obtained after the completion of each progressive optimization stage, corresponding to the wind power scenario forecasting problem for the day in Nov. 20th, 2013.

Table 4
Performance comparison of solution algorithms in scenario forecasting.

	ES	BS: Up-Ramp	BS: Down-Ramp	BS: Long-High	BS: Long-Low	PB
NSGA-II	1.902	0.165	0.176	0.116	0.150	1.303
NSGA-III	1.871	0.165	0.170	0.114	0.146	1.295
PO-NSGA-II	1.746	0.163	0.165	**0.107**	0.137	1.260
PO-NSGA-III	**1.691**	**0.162**	**0.163**	**0.107**	**0.133**	**1.251**

PO is used to denote the progressive optimization-based counterpart. The best scores are highlighted in bold.

networks using Adam optimizer with a mini-batch size of 8. Leaky-ReLU activation is used in our networks except for the last layer of G which uses Tanh activation instead to constrain the output within $[-1, 1]$. Then, the 8-objective optimization framework can be established according to Subsection 3.2.1, where we set the confidence factor $\beta = 1.0$ in model (7). As for the parameters of PO-NSGA-III, we adopt the simulated binary crossover and polynomial mutation, where the crossover rate α_1 and mutation rate α_2 are set as $\alpha_1 = 0.6$ and $\alpha_2 = 0.01$. To strike a balance between computational complexity and solution optimality, we ignore the first three lower resolution stages and divide the progressive optimization process into 6 stages $(2 \times 72, 2 \times 144, \cdots, 2 \times 2304)$. In each stage, the population size n_{pop} and maximum iteration n_{iter} are set as $n_{\text{pop}} = 120$ and $n_{\text{iter}} = 500$. To obtain a fair comparison, Chen's Method, Vine Copula and KDE use the settings suggested in their literature.

4.4. Simulation results

For scenario generation, we first verify the quality of overall scenarios achieved by the proposed GAN model in all resolution dimensions, where in this study the resolution starts from 2×9 to 2×2304. The generated samples are compared with the real samples that have similar patterns through Euclidean distance-based search, and the results are depicted in Fig. 6. It can be observed that with the increase of resolution, local curve details of the generated wind power scenarios are gradually refined and more complex temporal dynamic characteristics of randomness, volatility and intermittence are captured. In addition, the local wind power curve usually fluctuates violently, while the point forecast curve seems smoother. Fortunately, as shown in Fig. 6(b), our method can correctly identify and capture these two distinct patterns, thus enhancing the quality of the subsequent day-ahead scenario forecasting.

For scenario forecasting, Nov. 20th, 2013 is selected as the forecast day. Fig. 7 shows the objective value paths (pareto fronts in parallel coordinates) of pareto solutions obtained after the completion of each stage in the progressive optimization, in which the descriptions of resolution stage are marked in the upper right corner of the subfigures. One can see that in the low-resolution stages, the diversity of solutions is mainly considered in the optimization to broaden the search space and avoid the generated scenarios concentrating on a single pattern. As the stage continues, almost all objective values show a downward convergence, which demonstrates the efficacy and stability of PO-NSGA-III when solving the scenario forecasting problem. Furthermore, a quantitative performance analysis of solution algorithm is conducted to prove the scientific rationality of PO-NSGA-III, in which another prevailing multi-objective algorithm NSGA-II [44] acknowledged to outperform many other evolutionary algorithms by related investigations is selected as the baseline. According to the results presented in Table 4, it can be observed that for the scenario forecasting problem PO-NSGA-III performs slightly better in terms of three metrics, followed by PO-NSGA-II, whereas the performance of two original versions without progressive optimization (i.e. NSGA-III and NSGA-II) is relatively poor. For more intuitive comparison, the forecasted results and the corresponding 120 scenarios produced by our method, Chen's Method, Vine Copula and KDE, are plotted in Fig. 8. It is worth noting that $(2106, 2304]$ in the time-axis indicates the time horizon of the forecast day, before which $(0, 2016]$ represents the previous 7 days. In the proposed method and Chen's Method, optimization process is conducted according to the available data related to the forecast day, which is not necessary in sample-based methods like Vine Copula and KDE. It can be observed that the day-ahead point forecast data deviates from the realized wind power. In this case, the forecasted scenarios generated by three benchmark methods deviate from the realized wind power obviously due to the concentration on the inaccurate point forecast. By contrast, owing to the design of overall scenario structure, the temporal correlations between wind power and point forecast are captured in our method, thus resulting in forecasted scenarios following the actual trends better. In terms of the coverage on wind power realizations, scenarios produced by Chen's Method are most concentrated and can be thought of as the least conservative. This would forgo the reliability of power systems in favor of low costs when stochastic unit commitment is performed using the scenario set as input. Vine Copula and KDE, especially KDE, provide the most conservative (dispersed) scenarios that strongly favor higher reliability but increasing scheduling costs. Our method provides a balance between reliability and costs, which is more competitive and attractive for operators. As for the details of scenarios, the utilizing of PG-GAN enables us to produce more realistic wind power scenarios, especially in the curve turning and sudden changes. Moreover, by setting different initial population size of PO-NSGA-III, our method has the ability to produce scenarios with varied numbers, as shown in Fig. 9. This is very

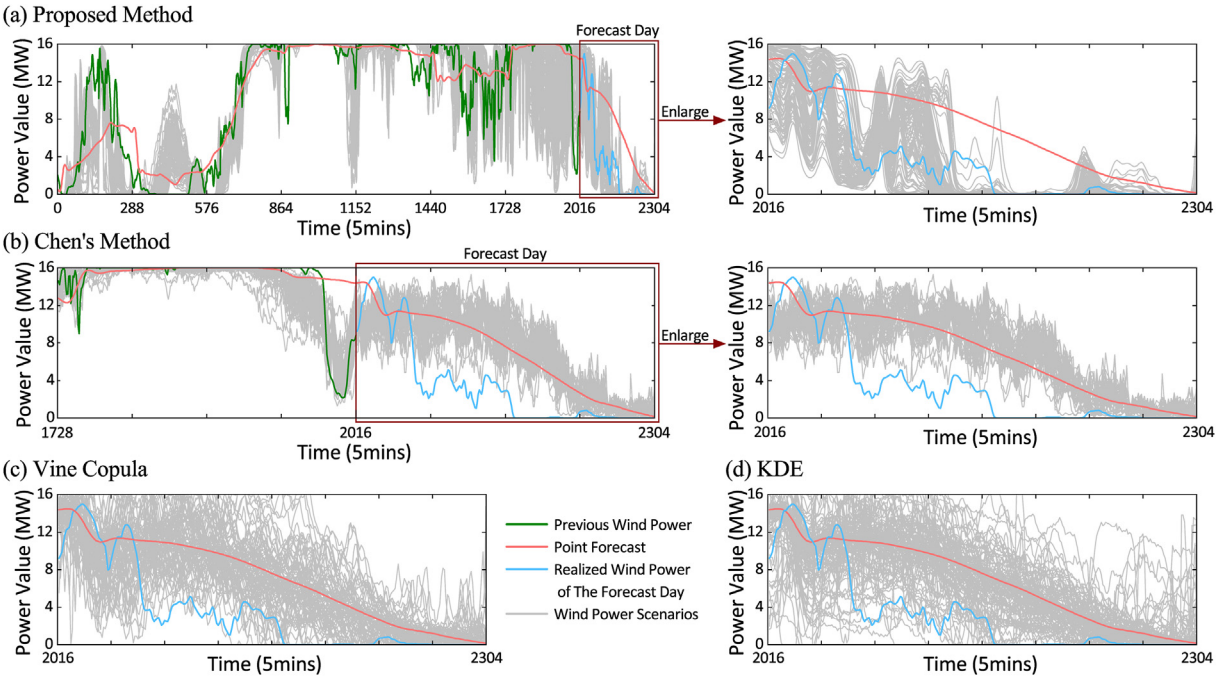

Fig. 8. Comparison of wind power scenario forecasting results (i.e. 120 forecasted scenarios for the day in Nov. 20th, 2013, gray solid line in time-axis of (2016, 2304]) using the proposed method (a), Chen's Method (b), Vine Copula (c) and KDE (d). Note that the complete optimization results related to the forecast day (including the matching results of wind power in previous days) are also given in the first two methods.

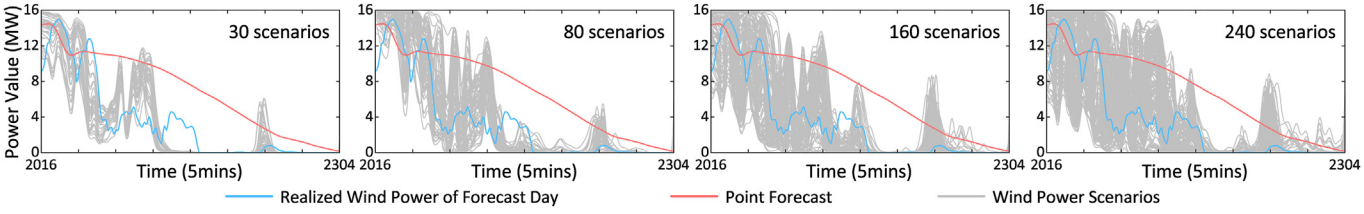

Fig. 9. Experimental results of 30, 80, 160 and 240 wind power scenarios for the day in Nov. 20th, 2013 produced by the proposed method.

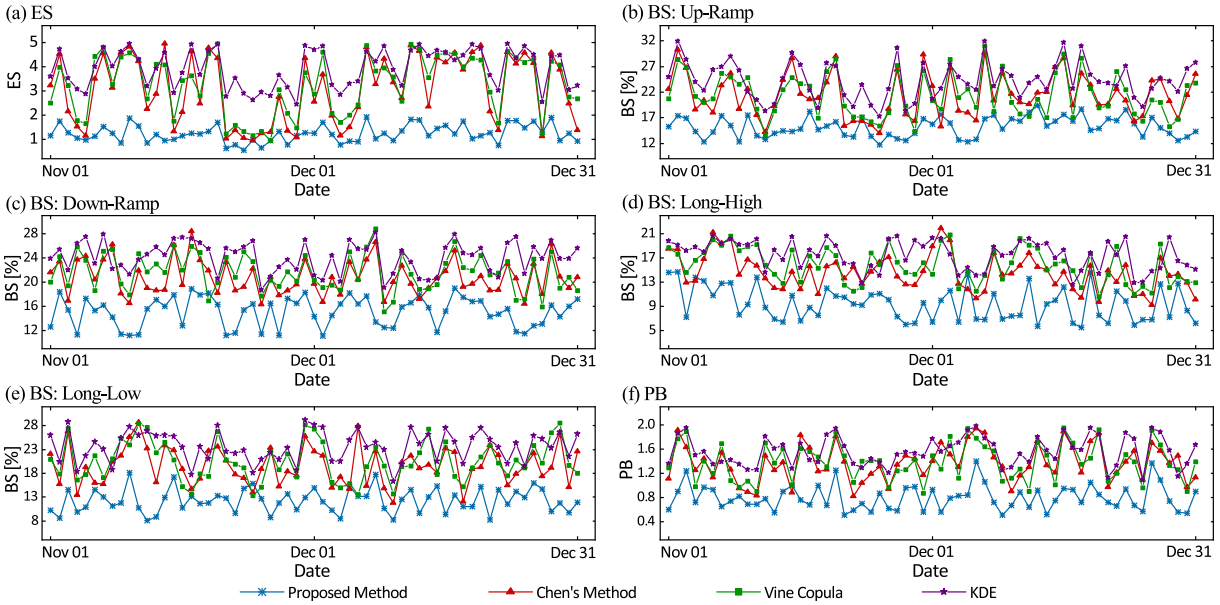

Fig. 10. Performance comparison between the proposed method and three benchmark methods on daily ES (a), BS defined by four events (b–e), and PB (f) metrics for wind power scenarios from Nov. 1st to Dec. 31st, 2013.

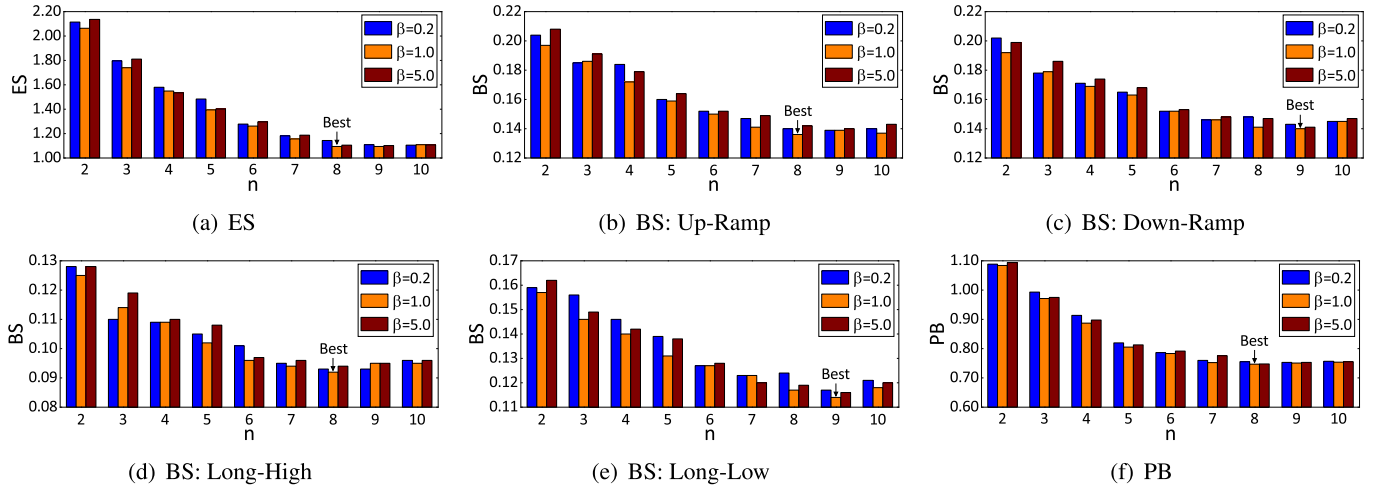

Fig. 11. Sensitive analysis for the proposed method on averaged ES (a), BS defined by four events (b–e) and PB (f) metrics under different settings of the consecutive days n and the confidence factor β.

important for the optimal decision-making of stochastic optimization and robust optimization, since a good scenario forecasting method should have the ability to generate different number of scenarios without sacrificing time efficiency, thereby can flexibly respond to the capturing requirements of actual different-scale wind power uncertainty as well as the low-probability extreme events. From the perspective of stochastic optimization, the full description of wind generation uncertainty benefits from large amounts of scenarios from which representative scenarios can be further refined by some reduction techniques to mitigate the computational burden. Providing fewer scenarios helps diminish the computational burden, but at the risk of power system reliability. From the perspective of robust optimization, the worst scenarios (i.e. extreme events) with low-probability are more likely to be found in a larger scenario set. Hence, the conservatism of optimal operations of power systems can be quantitatively controlled by the number of scenarios provided.

In order to make the comparison more convincing, all the test days from Nov. 1st to Dec. 31st, 2013 are evaluated based on the three metrics introduced in Subsection 4.2. Fig. 10(a) depicts the corresponding ES results. With exception to very few days (Nov. 24th, 26th, 29th and Dec. 27th, 2013), our method outperforms all benchmark methods because lower ES indicates better reliability and sharpness of wind power scenarios. The unsatisfactory performance of the proposed method in the above exceptions could be attributed to extreme patterns (e.g. 0 MW for a whole day) within consecutive days, which leads to the failure of identification and approximation in the optimization process. Fig. 10(b)–(e) provide the BS results considering the four events given in Table 2, which show the superiority of the proposed method in correctly matching the behaviors of the realized wind power in most test days. The scenarios provided by Chen's Method and Vine Copula prove to achieve competitive BS results in some test days, whereas the KDE-based scenarios fail to follow the correct profiles, thus affecting the performance. Besides, a similar conclusion on the PB metric can be obtained in Fig. 10(f), which proves that our method has better performance in reflecting the marginal distribution of actual wind power. In addition, the prediction performance of the three metrics on all test days has a smaller range of fluctuations, which shows that the proposed method is relatively robust.

Recall that all the experiments above were carried out under the same parameter setting ($n = 8$, $\beta = 1.0$). Then we also investigate how varied combinations of the consecutive days n and the confidence factor β affect the quality of forecasted scenarios. Nine n values from 2 to 10 and three typical β values (i.e., 0.2, 1.0 and 5.0) are selected, in total 27 combinations, to conduct the sensitive analysis. The averaged evaluation results of all test days on the three metrics are shown in the six subfigures of Fig. 11, wherein the best scores are marked. On the one hand, the prediction performance is significantly improved when increasing the consecutive days n from 2 to 8, however it reaches saturation or even worse when n is larger than 8. On the other hand, the setting of $\beta = 1.0$ performs the best when n is fixed. Moreover, it is noted that the runtime of the proposed method is affected by the value of n. Therefore, we implement the method with different n, and provide the runtime costs together with Chen's Method, Vine Copula and KDE in Table 5. It can be found that in this case study, the setting of $n = 8$ and $\beta = 1.0$ generates acceptable wind power scenarios considering both the evaluation metrics and time efficiency compared with three benchmark methods.

Table 5
Time efficiency comparison.

Number of scenarios	Time cost (s)											
	Proposed Method (with different settings of the consecutive days n)									Chen's Method	Vine Copula	KDE
	2	3	4	5	6	7	8	9	10			
30	15.01	19.90	25.62	31.32	47.56	69.89	97.26	131.22	182.42	110.28	90.86	122.46
80	16.28	22.17	29.65	50.41	71.30	100.45	134.70	192.65	292.54	196.50	123.04	129.75
160	18.16	25.87	34.82	61.30	98.69	136.25	180.83	286.04	405.32	522.63	198.41	140.70
240	22.64	31.51	48.33	78.01	123.36	181.94	245.02	373.74	527.36	924.34	282.17	155.21

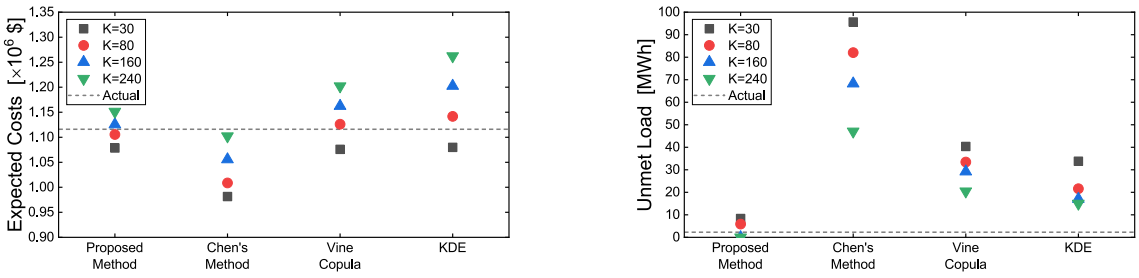

(a) Expected total costs (b) Unmet load amounts

Fig. 12. Results of expected total costs (a) and unmet load amounts (b) under the condition of different scenario numbers K when the proposed method and three benchmark methods are applied in a real day-head scheduling on IEEE RTS-96. Actual results that uses the wind power realization are plotted in gray dash lines.

4.5. Theoretical and practical significance

The uncertainty of wind power generation brings great challenges to the power system scheduling activities. One of the main ways to solve this problem is to provide accurate and reliable day-ahead wind power scenarios. In this sense, the theoretical and practical significance of this paper can be explained as follows.

From a theoretical point of view, by building a deep generative network and a multi-objective optimization framework, the proposed scenario forecasting method could learn the distribution of historical wind power data as well as point forecast data and capture their complex diurnal pattern correlations without any explicit probabilistic shape assumption, which not only enriches the theoretical foundation of wind power uncertainty representation that guarantees the operation safety of power systems, but also contributes to the development of data-driven uncertainty modeling theory in other engineering application realms.

From a practical point of view, a day-ahead power system scheduling problem that uses scenarios as input is considered to assess the performance of four scenario forecasting methods in practice. The experiments are performed on a modified test system IEEE RTS-96 available at [45], which consists of 73 buses, 96 generators and 19 wind farms. The forecasted wind power scenarios on Nov. 20th, 2013 are used, which are normalized and scaled in proportion according to the wind farm capacity. For simplicity, all geographically adjacent wind farms are postulated to share perfect positive correlation. The value of lost load is set as 1000 $/ MWh and the penalty of wind curtailment is ignored for simplicity. A two-stage stochastic unit commitment optimization incorporated by wind power uncertainty is executed to determine the day-ahead on/off status and production levels of thermal units. Fig. 12 compares the results of four methods on the expected total costs ($\times 10^6$ $) and the unmet load amounts (MWh) under the condition of different scenario numbers. Actual results (1.1218×10^6 $ and 2.4473 MWh, respectively) calculated on a deterministic unit commitment optimization using the wind power realization as input, are also given in Fig. 12. We observe that Chen's Method has lower costs but significant unmet load amounts, indicating the least conservatism of scenarios provided by Chen's Method, since they exclude some extreme events. Vine Copula and KDE alleviate the load shedding phenomena (i.e. lower unmet load amounts) at the expense of higher expected costs, due to the fact that their scenarios are relatively dispersed and able to encapsulate possible realizations. The costs of the proposed method are most in line with the actual costs and the unmet load amounts are lowest. The main reason is that our scenarios have a preciser representation of actual wind power trend and more realistic local details, thereby achieving better wind power uncertainty characterization and scheduling performance in practice.

5. Conclusions

High-quality scenario forecasting of renewable energy represented by wind power is significant for modern power system planning, management, and operations. However, this is a challenging task due to the intrinsic intermittence and fluctuation of wind energy. In this study, a novel multi-objective wind power scenario forecasting method based on PG-GAN was proposed to capture the nonlinear temporal dynamics and complex diurnal pattern correlations. It adopts an overall scenario structure which outputs the wind power scenario together with the corresponding point forecast scenario. Then the forecasting model was established to minimize several objectives so that the difference between the network outputs and available information of the forecast day can be reduced. Finally, the forecasting model was solved by PO-NSGA-III, and a relatively plausible scenario set that reflects all possible day-head wind power temporal trajectories could be obtained even in the case of inaccurate point forecast provided.

Experimental results based on a realistic case study demonstrate that the using of PG-GAN enriches the details of wind power scenarios, and the proposed forecasting model with the overall scenario structure achieves higher quality scenarios than the existing methods. Moreover, the method developed in this paper is also capable of generating different amounts of wind power scenarios without sacrificing time efficiency. Finally, the proposed method is data-driven and promising to solve a series of scenario forecasting problems in some other research realms. However, this study also suffers from several shortcomings: 1) the spatial dynamics of multiple wind farms are not considered. 2) the meteorological prediction information is neglected. In the future, we will make further improvements about the proposed scenario forecasting method by focusing on the above points and extend the method to more actual applications of power system operations.

Credit author statement

Ran Yuan: Methodology, Writing – original draft, Software. Bo Wang: Software, Resources, Writing – review & editing. Zhixin Mao: Investigation, Software. Junzo Watada: Writing – review & editing.

Declaration of competing interest

The authors declare that they have no known competing financial interests or personal relationships that could have appeared to influence the work reported in this paper.

Acknowledgement

This work was supported by the National Natural Science Foundation of China (Grant No. 61603176, 71732003), the Natural Science Foundation of Jiangsu Province (Grant No. BK20160632), and the Fundamental Research Funds for the Central Universities (Grant No. 14380037). The authors would like to express their gratitude to the anonymous reviewers, whose helpful comments and suggestions were advantageous to improve the quality of this paper.

References

[1] Ren G, Wan J, Liu J, Yu D. Spatial and temporal correlation analysis of wind power between different provinces in China. Energy 2020;191:116514.
[2] Buhan S, Özkazanç Y, Çadırcı I. Wind pattern recognition and reference wind mast data correlations with NWP for improved wind-electric power forecasts. IEEE Transactions on Industrial Informatics 2016;12(3):991–1004.
[3] Zhang Y, Li Y, Zhang G. Short-term wind power forecasting approach based on Seq2Seq model using NWP data. Energy; 2020a. p. 118371.
[4] Li X, Jiang C. Short-term operation model and risk management for wind power penetrated system in electricity market. IEEE Trans Power Syst 2010;26(2):932–9.
[5] Duan J, Wang P, Ma W, Tian X, Fang S, Cheng Y, Chang Y, Liu H. Short-term wind power forecasting using the hybrid model of improved variational mode decomposition and correntropy long short-term memory neural network. Energy; 2020. p. 118980.
[6] Quan H, Srinivasan D, Khosravi A. Short-term load and wind power forecasting using neural network-based prediction intervals. IEEE Transactions on Neural Networks and Learning Systems 2013;25(2):303–15.
[7] Zhang Y, Wang J, Wang X. Review on probabilistic forecasting of wind power generation. Renew Sustain Energy Rev 2014;32:255–70.
[8] Pinson P, Madsen H, Nielsen HA, Papaefthymiou G, Klöckl B. From probabilistic forecasts to statistical scenarios of short-term wind power production. Wind Energy 2009;12(1):51–62.
[9] Osório G, Lujano-Rojas J, Matias J, Catalão J. A new scenario generation-based method to solve the unit commitment problem with high penetration of renewable energies. Int J Electr Power Energy Syst 2015;64:1063–72.
[10] Xu J, Wang B, Sun Y, Xu Q, Liu J, Cao H, Jiang H, Lei R, Shen M. A day-ahead economic dispatch method considering extreme scenarios based on wind power uncertainty. CSEE Journal of Power and Energy Systems 2019;5(2):224–33.
[11] Goodfellow I, Pouget-Abadie J, Mirza M, Xu B, Warde-Farley D, Ozair S, Courville A, Bengio Y. Generative adversarial nets. In: Advances in neural information processing systems; 2014. p. 2672–80.
[12] Karras T, Aila T, Laine S. J. Lehtinen, progressive growing of GANs for improved quality, stability, and variation. In: International conference on learning representations; 2018.
[13] Deb K, Jain H. An evolutionary many-objective optimization algorithm using reference-point-based nondominated sorting approach, part I: solving problems with box constraints. IEEE Trans Evol Comput 2013;18(4):577–601.
[14] Ma X-Y, Sun Y-Z, Fang H-L. Scenario generation of wind power based on statistical uncertainty and variability. IEEE Transactions on Sustainable Energy 2013;4(4):894–904.
[15] Morales JM, Minguez R, Conejo AJ. A methodology to generate statistically dependent wind speed scenarios. Appl Energy 2010;87(3):843–55.
[16] Bessa RJ, Miranda V, Botterud A, Zhou Z, Wang J. Time-adaptive quantile-copula for wind power probabilistic forecasting. Renew Energy 2012a;40(1):29–39.
[17] Becker R. Generation of time-coupled wind power infeed scenarios using pair-copula construction. IEEE Transactions on Sustainable Energy 2017;9(3):1298–306.
[18] Wang Z, Wang W, Liu C, Wang Z, Hou Y. Probabilistic forecast for multiple wind farms based on regular vine copulas. IEEE Trans Power Syst 2017;33(1):578–89.
[19] Wang Y, Liu Y, Kirschen DS. Scenario reduction with submodular optimization. IEEE Trans Power Syst 2016;32(3):2479–80.
[20] Hu J, Li H. A new clustering approach for scenario reduction in multi-stochastic variable programming. IEEE Trans Power Syst 2019;34(5):3813–25.
[21] Li J, Lan F, Wei H. A scenario optimal reduction method for wind power time series. IEEE Trans Power Syst 2015;31(2):1657–8.
[22] Vagropoulos SI, Kardakos EG, Simoglou CK, Bakirtzis AG, Catalao JP. ANN-based scenario generation methodology for stochastic variables of electric power systems. Elec Power Syst Res 2016;134:9–18.
[23] Cui M, Ke D, Sun Y, Gan D, Zhang J, Hodge B-M. Wind power ramp event forecasting using a stochastic scenario generation method. IEEE Transactions on Sustainable Energy 2015;6(2):422–33.
[24] Xu Y, Shi L, Ni Y. Deep-learning-based scenario generation strategy considering correlation between multiple wind farms. J Eng 2017;2017(13):2207–10.
[25] Sideratos G, Hatziargyriou ND. Probabilistic wind power forecasting using radial basis function neural networks. IEEE Trans Power Syst 2012;27(4):1788–96.
[26] Chen J, Rabiti C. Synthetic wind speed scenarios generation for probabilistic analysis of hybrid energy systems. Energy 2017;120:507–17.
[27] Chen Y, Wang Y, Kirschen D, Zhang B. Model-free renewable scenario generation using generative adversarial networks. IEEE Trans Power Syst 2018a;33(3):3265–75.
[28] Chen Y, Li P, Zhang B. Bayesian renewables scenario generation via deep generative networks. In: 2018 52nd annual conference on information sciences and systems (CISS). IEEE; 2018b. p. 1–6.
[29] Jiang C, Mao Y, Chai Y, Yu M, Tao S. Scenario generation for wind power using improved generative adversarial networks. IEEE Access 2018;6:62193–203.
[30] Wei H, Hongxuan Z, Yu D, Yiting W, Ling D, Ming X. Short-term optimal operation of hydro-wind-solar hybrid system with improved generative adversarial networks. Appl Energy 2019;250:389–403.
[31] Chen Y, Wang X, Zhang B. An unsupervised deep learning approach for scenario forecasts. In: 2018 power systems computation conference (PSCC). IEEE; 2018c. p. 1–7.
[32] Wang F, Zhang Z, Liu C, Yu Y, Pang S, Duić N, Shafie-Khah M, Catalão JP. Generative adversarial networks and convolutional neural networks based weather classification model for day ahead short-term photovoltaic power forecasting. Energy Convers Manag 2019;181:443–62.
[33] Zhang Y, Ai Q, Xiao F, Hao R, Lu T. Typical wind power scenario generation for multiple wind farms using conditional improved Wasserstein generative adversarial network. Int J Electr Power Energy Syst 2020b;114:105388.
[34] Liang J, Tang W. Sequence generative adversarial networks for wind power scenario generation. IEEE J Sel Area Commun 2019;38(1):110–8.
[35] Zhu J-Y, Park T, Isola P, Efros AA. Unpaired image-to-image translation using cycle-consistent adversarial networks. In: Proceedings of the IEEE international conference on computer vision; 2017. p. 2223–32.
[36] Yu L, Zhang W, Wang J, Yu Y. Seqgan: sequence generative adversarial nets with policy gradient. In: Thirty-first AAAI conference on artificial intelligence; 2017.
[37] Aly HH. A novel deep learning intelligent clustered hybrid models for wind speed and power forecasting. Energy 2020;213:118773.
[38] M. Arjovsky, L. Bottou, Towards principled methods for training generative adversarial networks, arXiv preprint arXiv:1701.04862.
[39] Draxl C, Clifton A, Hodge B-M, McCaa J. The wind integration national dataset (wind) toolkit. Appl Energy 2015;151:355–66.
[40] Bessa RJ, Miranda V, Botterud A, Wang J, Constantinescu EM. Time adaptive conditional kernel density estimation for wind power forecasting. IEEE Transactions on Sustainable Energy 2012b;3(4):660–9.
[41] Staid A, Watson J-P, Wets RJ-B, Woodruff DL. Generating short-term probabilistic wind power scenarios via nonparametric forecast error density estimators. Wind Energy 2017;20(12):1911–25.
[42] Pinson P, Girard R. Evaluating the quality of scenarios of short-term wind power generation. Appl Energy 2012;96:12–20.
[43] P. Muniain, F. Ziel, Probabilistic forecasting in day-ahead electricity markets: simulating peak and off-peak prices, Int J Forecast .
[44] Deb K, Pratap A, Agarwal S, Meyarivan T. A fast and elitist multiobjective genetic algorithm: NSGA-II. IEEE Trans Evol Comput 2002;6(2):182–97.
[45] H. Pandzic, Y. Dvorkin, T. Qiu, Y. Wang, D. Kirschen, Unit commitment under uncertainty-GAMS models, Library of the Renewable Energy Analysis Lab (REAL), University of Washington, Seattle, USA .